

# Eigenvalue-corrected Natural Gradient Based on a New Approximation

Kai-Xin Gao<sup>1\*</sup>, Xiao-Lei Liu<sup>1\*</sup>, Zheng-Hai Huang<sup>1\*</sup>, Min Wang<sup>2</sup>,  
Shuangling Wang<sup>2</sup>, Zidong Wang<sup>2</sup>, Dachuan Xu<sup>3†</sup>, Fan Yu<sup>2</sup>

<sup>1</sup> School of Mathematics, Tianjin University

<sup>2</sup> Central Software Institute, Huawei Technologies

<sup>3</sup> Department of Operations Research and Information Engineering, Beijing University of Technology

## Abstract

Using second-order optimization methods for training deep neural networks (DNNs) has attracted many researchers. A recently proposed method, Eigenvalue-corrected Kronecker Factorization (EKFAC) (George et al., 2018), proposes an interpretation of viewing natural gradient update as a diagonal method, and corrects the inaccurate re-scaling factor in the Kronecker-factored eigenbasis. Gao et al. (2020) considers a new approximation to the natural gradient, which approximates the Fisher information matrix (FIM) to a constant multiplied by the Kronecker product of two matrices and keeps the trace equal before and after the approximation. In this work, we combine the ideas of these two methods and propose Trace-restricted Eigenvalue-corrected Kronecker Factorization (TEKFAC). The proposed method not only corrects the inexact re-scaling factor under the Kronecker-factored eigenbasis, but also considers the new approximation method and the effective damping technique proposed in Gao et al. (2020). We also discuss the differences and relationships among the Kronecker-factored approximations. Empirically, our method outperforms SGD with momentum, Adam, EKFAC and TKFAC on several DNNs.

## 1 Introduction

Deep learning has made significant progress in various natural language and computer vision applications. But as models becoming more and more complex, deep neural networks (DNNs) usually have huge parameters (for example, VGG16 has over 1.5 million

---

\*Equal contribution

†Corresponding author, Email: xudc@bjut.edu.cn

parameters) to be trained, which takes a long time. Therefore, the research of more efficient optimization algorithms has attracted many researchers.

Among the algorithms for training DNNs, the most popular and widely used method is Stochastic Gradient Descent (SGD) (Robbins and Monro, 1951). During training, the goal of SGD is to find the optimal parameters  $\omega$  to minimize the objective function  $h(\omega)$ . The parameters  $\omega$  are updated by:  $\omega \leftarrow \omega - \eta \nabla_{\omega} h$ , where  $\eta$  is the learning rate. To achieve better training performance, many variants of SGD also have been proposed, such as momentum (Qian, 1999), Nesterov’s acceleration (Nesterov, 1983) and etc. However, SGD only considers first-order gradient information, which leads to some deficiencies, including relatively-slow convergence and sensitivity to hyper-parameter settings.

To avoid these problems, the second-order optimization algorithm may be a good choice. More importantly, second-order optimization algorithms can greatly accelerate convergence by using curvature matrix to correct gradient through training. The parameters update rule is:  $\omega \leftarrow \omega - \eta F^{-1} \nabla_{\omega} h$ , where  $F^{-1}$  is the inverse of curvature matrix. The curvature matrix  $F$  is defined differently in second-order optimization algorithms. For Newton’s method,  $F$  is the Hessian matrix which represents second-order derivatives. For natural gradient method (Amari, 1998),  $F$  is the Fisher information matrix (FIM) which represents covariance of second-order gradient statistics. However, the curvature matrix and its inverse dramatically increase computing and storage costs. It is impractical to compute and invert an exact curvature matrix directly. Therefore, many approximate methods have been proposed.

A simple but crude method is diagonal approximation, such as AdaGrad (Duchi et al., 2011), RMSprop (Tieleman and Hinton, 2012), Adam (Kingma and Ba, 2014) and etc. These algorithms are computationally tractable but lose much curvature matrix information. More elaborate algorithms are no longer limited to diagonal approximation. For Newton’s methods, quasi-Newton method (Dennis and Moré, 1977; Le et al., 2011; Berahas et al., 2019; Goldfarb et al., 2020) can be used to approximate the Hessian matrix and its advantages over Newton’s method is that the Hessian matrix does not need to be inverted directly. Hessian-Free optimization approach (Martens, 2010; Kiros, 2013; Pan et al., 2017) provides a matrix-free conjugate-gradient algorithm for approximating the Hessian matrix. For natural gradient methods, Kronecker-factored Approximate Curvature (KFAC) (Martens and Grosse, 2015) presents efficient block diagonal approximation and block tri-diagonal approximation of the FIM in fully-connected neural networks. This method has been further extended to convolutional neural networks (Grosse and Martens, 2016), recurrent neural networks (Martens et al., 2018) and variational Bayesian neural networks (Bae et al., 2018; Zhang et al., 2018). KFAC has also been used in large-scale distributed computing for deep neural networks (Ba et al., 2017; Osawa et al., 2019; Pauloski et al., 2020; Yang et al., 2020).

In particular, George et al. (2018) proposes a new explanation for the natural gradient update, in which the natural gradient update is viewed as diagonal method in Kronecker-factored eigenbasis. And under this interpretation, the re-scaling factor under the KFAC eigenbasis is not exact. So Eigenvalue-corrected Kronecker Factorization

(EKFAC) is proposed to correct the inaccurate re-scaling factor. Recently, [Gao et al. \(2020\)](#) adopts a new model to approximate the FIM called Trace-restricted Kronecker Factorization (TKFAC). TKFAC approximates the FIM as a constant multiple of the Kronecker product of two matrices. In experiments, TKFAC has better performance than KFAC. Therefore, it is natural for us to consider the TKFAC’s model under the interpretation proposed in EKFAC.

In this work, we combine the ideas of EKFAC and TKFAC, then present Trace-restricted Eigenvalue-corrected Kronecker Factorization (TEKFAC). Our contribution can be summarized as follows:

- Instead of approximating FIM to the Kronecker product of two smaller matrices, we consider EKFAC based on the approximation model adopted by TKFAC. So, we change the Kronecker-factored eigenbasis in EKFAC and propose TEKFAC, which not only corrects the inexact re-scaling factor but also takes the advantages of TKFAC.
- We discuss the relationships and differences among the several methods, including KFAC, EKFAC, TKFAC and TEKFAC. Empirically, we compare TEKFAC with SGD with momentum (SGDM), Adam, EKFAC and TKFAC using the SVHN, CIFAR-10 and CIFAR-100 datasets on VGG16 and ResNet20. Our method has more excellent performance than these baselines.

## 2 Methods to Approximate the Natural Gradient

### 2.1 Natural Gradient

During the training process of DNNs, the purpose is to minimize a loss function  $h(\omega)$ . Throughout this paper, we use  $\mathbb{E}[\cdot]$  to represent the mean of the samples  $(x, y)$  and the cross-entropy loss function is computed as

$$h(\omega) = \mathbb{E}[-\log p(y|x, \omega)],$$

where  $\omega$  is a vector of parameters,  $x$  is the input,  $y$  is the label, and  $p(y|x, \omega)$  represents the density function of the neural network’s predictive distribution  $P_{y|x}(\omega)$ .

Natural gradient was first proposed by [Amari \(1998\)](#). It gives the steepest descent direction in the distribution space rather than the space of parameters. In distribution space, the distance between two distributions  $P(\omega)$  and  $P(\omega + \Delta\omega)$  is measured by the K-L divergence:  $D_{\text{KL}}(P(\omega)||P(\omega + \Delta\omega)) \approx \frac{1}{2}\omega^\top F\omega$ , where  $F$  is the FIM, and is defined as

$$F = \mathbb{E}[\nabla_\omega \log p(y|x, \omega) \nabla_\omega \log p(y|x, \omega)^\top]. \quad (2.1)$$

The natural gradient is usually defined as  $F^{-1}\nabla_\omega h$ , and it provides the update direction for natural gradient descent. So, the parameters are updated by

$$\omega \leftarrow \omega - \eta F^{-1} \nabla_\omega h, \quad (2.2)$$

where  $\eta$  is the learning rate.

## 2.2 KFAC

For DNNs which have millions or even billions of parameters, it is impractical to compute the exact FIM and its inverse matrix. KFAC provides an useful approximation. Consider a DNN with  $L$  layers and denote the inputs  $a_{l-1}$  which are the activations of the previous layer, outputs  $s_l$ , and weight  $W_l$  for the  $l$ -th layer. Then, we have  $s_l = W_l a_{l-1}$ . For simplicity, we will use the following notation:

$$\mathcal{D}t := \nabla_t \log p(y|x, \omega), u_l := \mathcal{D}s_l,$$

where  $t$  is an arbitrary parameter. Therefore, the gradient of weight is  $\mathcal{D}W_l = a_{l-1} u_l$ , and the Eq. (2.1) can be written as  $F = \mathbb{E}[\mathcal{D}\omega \mathcal{D}\omega^\top]$ .

Firstly, KFAC approximates the FIM  $F$  as a block diagonal matrix

$$F \approx \text{diag}(F_1, F_2, \dots, F_L) = \text{diag}(\mathbb{E}[\mathcal{D}\omega_1 \mathcal{D}\omega_1^\top], \mathbb{E}[\mathcal{D}\omega_2 \mathcal{D}\omega_2^\top], \dots, \mathbb{E}[\mathcal{D}\omega_L \mathcal{D}\omega_L^\top]), \quad (2.3)$$

where  $\omega_l = \text{vec}(W_l)$  for any  $l \in \{1, 2, \dots, L\}$ .

Then, each block matrix of the FIM can be written as

$$F_l = \mathbb{E}[\mathcal{D}\omega_l \mathcal{D}\omega_l^\top] = \mathbb{E}[(a_{l-1} \otimes u_l)(a_{l-1} \otimes u_l)^\top] \approx \mathbb{E}[a_{l-1}^\top a_{l-1}] \otimes \mathbb{E}[u_l^\top u_l] = A_{l-1} \otimes U_l, \quad (2.4)$$

where  $\otimes$  represents the Kronecker product,  $A_{l-1} = \mathbb{E}[a_{l-1} a_{l-1}^\top]$  and  $U_l = \mathbb{E}[u_l u_l^\top]$ . Due to the properties of Kronecker product  $(A_{l-1} \otimes U_l)^{-1} = A_{l-1}^{-1} \otimes U_l^{-1}$  and  $(A_{l-1} \otimes U_l) \text{vec}(X) = \text{vec}(U_l X A_{l-1}^\top)$  for any matrix  $X$ , decomposing  $F_l$  into  $A_{l-1}$  and  $U_l$  not only saves the cost of storing and inverting the exact FIM, but also enables tractable methods to compute the approximate natural gradient

$$(A_{l-1} \otimes U_l)^{-1} \nabla_{\omega_l} h = (A_{l-1} \otimes U_l)^{-1} \text{vec}(\nabla_{W_l} \phi) = \text{vec}(U_l^{-1} (\nabla_{W_l} \phi) A_{l-1}^{-1}).$$

## 2.3 EKFac

George et al. (2018) proposes an other interpretation of the natural gradient update  $F^{-1} \nabla_{\omega} h$ . Let  $F = Q_F \Lambda_F Q_F^\top$  be the eigendecomposition of the FIM, where  $\Lambda$  is a diagonal matrix with eigenvalues and  $Q$  is an orthogonal matrix whose columns correspond to eigenvectors. Then, the natural gradient update will be

$$F^{-1} \nabla_{\omega} h = \underbrace{Q_F}_{(c)} \underbrace{\Lambda_F^{-1} Q_F^\top \nabla_{\omega} h}_{(a)}. \quad (2.5)$$

The Eq. (2.5) can be explained by three steps: (a) multiplying  $\nabla_{\omega} h$  by  $Q_F^\top$ , which projects the gradient vector  $\nabla_{\omega} h$  to the eigenbasis  $Q_F$ ; (b) multiplying by the diagonal matrix  $\Lambda_F$ , which re-scales the coordinates in that eigenbasis by the diagonal inverse

matrix  $\Lambda_F^{-1}$ ; (c) multiplying by  $Q_F$ , which projects the re-scaled coordinates back to the initial basis. The re-scaling factor can be computed by  $(\Lambda_F)_{ii} = \mathbb{E}[(Q_F^\top \nabla_\omega h)_i^2]$ , whose entries are the second moment of the vector  $Q_F^\top \nabla_\omega h$  (the gradient vector in the eigenbasis). Under this interpretation, for a diagonal approximation of the FIM, the re-scaling factor is  $(\Lambda_F)_{ii} = \mathbb{E}[(\nabla_\omega h)_i^2]$  and the eigenbasis can be chosen as the identity matrix  $I$ . Although the re-scaling factor is efficient, obtaining an exact eigenbasis is difficult, the eigenbasis  $I$  is too crude which leads to great approximation error.

KFAC decomposes the FIM  $F$  into two Kronecker factors  $A_{l-1}$  and  $U_l$ . Because  $A_{l-1}$  and  $U_l$  are real symmetric positive semi-definite matrices, they can be expressed as  $A_{l-1} = Q_{A_{l-1}} \Lambda_{A_{l-1}} Q_{A_{l-1}}^\top$  and  $U_l = Q_{U_l} \Lambda_{U_l} Q_{U_l}^\top$  by eigendecomposition. By the property of Kronecker product, Eq. (2.4) can be written as

$$\begin{aligned} F_l &\approx A_{l-1} \otimes U_l = (Q_{A_{l-1}} \Lambda_{A_{l-1}} Q_{A_{l-1}}^\top) \otimes (Q_{U_l} \Lambda_{U_l} Q_{U_l}^\top) \\ &= (Q_{A_{l-1}} \otimes Q_{U_l}) (\Lambda_{A_{l-1}} \otimes \Lambda_{U_l}) (Q_{A_{l-1}} \otimes Q_{U_l})^\top. \end{aligned} \quad (2.6)$$

According to this interpretation,  $Q_{A_{l-1}} \otimes Q_{U_l}$  gives the eigenbasis of the Kronecker product  $A_{l-1} \otimes U_l$ . Compared with diagonal approximations, KFAC provides a more exact eigenbasis approximation of the full FIM eigenbasis. However, the re-scaling factor is not accurate under the KFAC eigenbasis, that is  $(\Lambda_{A_{l-1}} \otimes \Lambda_{U_l})_{ii} \neq \mathbb{E}[(Q_{A_{l-1}} \otimes Q_{U_l})^\top \nabla_{\omega_l} h)_i^2]$ . EKFACT corrects this inexact re-scaling factor by defining

$$(\Lambda_l^*)_{ii} = \mathbb{E}[(Q_{A_{l-1}} \otimes Q_{U_l})^\top \nabla_{\omega_l} h)_i^2].$$

Then,  $F_l$  can be approximated as

$$F_l \approx (Q_{A_{l-1}} \otimes Q_{U_l}) \Lambda_l^* (Q_{A_{l-1}} \otimes Q_{U_l})^\top. \quad (2.7)$$

## 2.4 TKFAC

Recently, Gao et al. (2020) proposed a new approximation of  $F_l$ , which approximates  $F_l$  as a Kronecker product scaled by a coefficient  $\sigma_l$ , i.e.,

$$F_l \approx \sigma_l \Phi_l \otimes \Psi_l, \quad (2.8)$$

where  $0 < \sigma_l < \infty$  is an unknown parameter,  $\Phi_l$  and  $\Psi_l$  are two unknown matrices with known traces. Denote  $\Lambda_{l-1} = a_{l-1} a_{l-1}^\top$  and  $\Gamma_l = u_l u_l^\top$ . Then, the factors in Eq. (2.8) can be computed by

$$\sigma_l = \frac{\mathbb{E}[\text{tr}(\Lambda_{l-1}) \text{tr}(\Gamma_l)]}{\text{tr}(\Phi_l) \text{tr}(\Psi_l)}, \quad \Phi_l = \frac{\text{tr}(\Phi_l) \mathbb{E}[\text{tr}(\Gamma_l) \Lambda_{l-1}]}{\mathbb{E}[\text{tr}(\Lambda_{l-1}) \text{tr}(\Gamma_l)]}, \quad \Psi_l = \frac{\text{tr}(\Psi_l) \mathbb{E}[\text{tr}(\Lambda_{l-1}) \Gamma_l]}{\mathbb{E}[\text{tr}(\Lambda_{l-1}) \text{tr}(\Gamma_l)]}. \quad (2.9)$$

An important property of TKFAC is to keep the traces equal, i.e.,  $\text{tr}(F_l) = \text{tr}(\sigma_l \Phi_l \otimes \Psi_l) = \sigma_l \text{tr}(\Phi_l) \text{tr}(\Psi_l)$ . Theoretically, the upper bound of TKFAC's approximation error is smaller than KFAC in general cases. What's more, experimental results show that

TKFAC can keep smaller approximation error than KFAC during training. In practice, to reduce computing costs, we can assume that  $\text{tr}(\Phi_l) = \text{tr}(\Psi_l) = 1$ . So, Eq. (2.9) can be simplified as

$$\sigma_l = \mathbb{E}[\text{tr}(\Lambda_{l-1})\text{tr}(\Gamma_l)], \quad \Phi_l = \frac{\mathbb{E}[\text{tr}(\Gamma_l)\Lambda_{l-1}]}{\mathbb{E}[\text{tr}(\Lambda_{l-1})\text{tr}(\Gamma_l)]}, \quad \Psi_l = \frac{\mathbb{E}[\text{tr}(\Lambda_{l-1})\Gamma_l]}{\mathbb{E}[\text{tr}(\Lambda_{l-1})\text{tr}(\Gamma_l)]}. \quad (2.10)$$

## 3 Methods

### 3.1 TEKFAC

EKFAC corrects the inexact re-scaling factor in KFAC based on the model that  $F_l$  is approximated the Kronecker product of two smaller matrices. If we think of TKFAC in terms of the interpretation adopted by EKFAC, the re-scaling factor in TKFAC is also inexact. So, in this section, we combine the ideas of these two methods and propose a new method called TEKFAC, which can keep track of the diagonal variance in TKFAC eigenbasis.

TKFAC approximates  $F_l$  as a Kronecker product of two factors  $\Phi_l, \Psi_l$  and scaled by the coefficient  $\sigma_l$ . It is easy to know that  $\Phi_l$  and  $\Psi_l$  are symmetric positive semi-definite matrices, according to eigendecomposition, we can obtain

$$\begin{aligned} F_l &\approx \sigma_l \Phi_l \otimes \Psi_l = \sigma_l (Q_{\Phi_l} \Lambda_{\Phi_l} Q_{\Phi_l}^\top) \otimes (Q_{\Psi_l} \Lambda_{\Psi_l} Q_{\Psi_l}^\top) \\ &= \sigma_l (Q_{\Phi_l} \otimes Q_{\Psi_l}) (\Lambda_{\Phi_l} \otimes \Lambda_{\Psi_l}) (Q_{\Phi_l} \otimes Q_{\Psi_l})^\top, \end{aligned} \quad (3.1)$$

where  $\Lambda_{\Phi_l}, \Lambda_{\Psi_l}$  are two diagonal matrices with eigenvalues of  $\Phi_l, \Psi_l$  and  $Q_{\Phi_l}, \Lambda_{\Phi_l}$  are two orthogonal matrices whose columns are eigenvectors of  $\Phi_l, \Psi_l$ , respectively. As the interpretation in subsection 3.2,  $Q_{\Phi_l} \otimes Q_{\Psi_l}$  gives the TKFAC eigenbasis, and the re-scaling factor can be selected as  $\sigma_l (\Lambda_{\Phi_l} \otimes \Lambda_{\Psi_l})$ . However, this re-scaling factor is also not guaranteed to match the second moment of the gradient vector in TKFAC eigenbasis, that is  $(\Lambda_{\Phi_l} \otimes \Lambda_{\Psi_l})_{ii} \neq \mathbb{E}[(Q_{\Phi_l} \otimes Q_{\Psi_l})^\top \nabla_{\omega_l} h]_i^2$ . Therefore, combined with the idea of EKFAC, we redefine the re-scaling factor by

$$(\Theta_l)_{ii} = \mathbb{E}[(Q_{\Phi_l} \otimes Q_{\Psi_l})^\top \nabla_{\omega_l} h]_i^2, \quad (3.2)$$

where  $\Theta_l$  is a diagonal matrix. Eq. (3.2) defines a more accurate re-scaling factor. Then, we can obtain the new approximation defined as follows

$$F_l \approx (Q_{\Phi_l} \otimes Q_{\Psi_l}) \Theta_l (Q_{\Phi_l} \otimes Q_{\Psi_l})^\top. \quad (3.3)$$

Similar to the analysis process of EKFAC, we can proof that  $\Theta_l$  is the optimal diagonal scaling factor under the TKFAC eigenbasis. That is  $\Theta_l$  is the optimal solution to the following problem.

$$\min_{\Lambda_l} \quad \|F_l - (Q_{\Phi_l} \otimes Q_{\Psi_l}) \Lambda_l (Q_{\Phi_l} \otimes Q_{\Psi_l})^\top\|_F$$

s.t.  $\Lambda_l$  is a diagonal matrix

According to this conclusion, we can easily prove the following theorem. For simplicity, we omit the subscript in the following theorem.

**Theorem 3.1.** *Let  $F_{\text{TKFAC}}$  and  $F_{\text{TEKFAC}}$  are the approximate matrices of the FIM  $F$ , i.e.,*

$$\begin{aligned} F_{\text{TKFAC}} &= (Q_\Phi \otimes Q_\Psi)(\sigma\Lambda_\Phi \otimes \Lambda_\Psi)(Q_\Phi \otimes Q_\Psi)^\top, \\ F_{\text{TEKFAC}} &= (Q_\Phi \otimes Q_\Psi)\Theta(Q_\Phi \otimes Q_\Psi)^\top, \end{aligned}$$

then, we have  $\|F - F_{\text{TEKFAC}}\|_F \leq \|F - F_{\text{TKFAC}}\|_F$ .

*Proof.* Because

$$\Theta = \arg \min_{\Lambda} \|F - (Q_\Phi \otimes Q_\Psi)\Lambda(Q_\Phi \otimes Q_\Psi)^\top\|_F$$

and for the diagonal matrices  $\Lambda_\Phi \otimes \Lambda_\Psi$ ,  $\Theta_l$

$$(\Lambda_\Phi \otimes \Lambda_\Psi)_{ii} \neq \mathbb{E}[(Q_\Phi \otimes Q_\Psi)^\top \nabla_\omega h_i]^2 = \Theta_{ii}.$$

Therefore, we have

$$\|F - (Q_\Phi \otimes Q_\Psi)\Theta(Q_\Phi \otimes Q_\Psi)^\top\|_F \leq \|F - (Q_\Phi \otimes Q_\Psi)(\sigma\Lambda_\Phi \otimes \Lambda_\Psi)(Q_\Phi \otimes Q_\Psi)^\top\|_F$$

that is

$$\|F - F_{\text{TEKFAC}}\|_F \leq \|F - F_{\text{TKFAC}}\|_F.$$

The proof is complete.  $\square$

So, TEKFAC provides a more accurate approximation for the FIM than TKFAC in theory. To use the second-order optimization methods effectively in practice, a suitable damping technique is also necessary. Crucially, powerful second-order optimizers like KFAC and EKFC usually require more complicated damping techniques, otherwise, they will tend to fail completely. KFAC introduces an effective damping technique by adding  $\sqrt{\lambda}I$  to the Kronecker factors  $A_{l-1}$  and  $U_l$ . In EKFC, since the re-scaling factor has been revised and redefined, it is no longer useful to add damping to the Kronecker factors, and the damping should be added to the re-scaling factor. TKFAC adopts the same damping technique as KFAC for FNNs and proposes a new automatic tuning damping for CNNs. For TEKFAC, we also use the same damping technique as EKFC for FNNs and the new damping technique adopted in TKFAC for CNNs, i.e.,

$$F_l \approx (Q_{\Phi_l} \otimes Q_{\Psi_l})(\Theta_l + \lambda I)(Q_{\Phi_l} \otimes Q_{\Psi_l})^\top \quad (3.4)$$

where  $\lambda$  is a reasonably large positive scalar for FNNs and

$$\lambda = \frac{\max\{\text{tr}(\Theta_l), \vartheta\}}{\dim(\Theta_l)} \quad (3.5)$$

for CNNs. In Eq. (3.5),  $\vartheta$  is a reasonably large positive scalar and  $\dim$  denotes the number of the rows (or columns) of  $\Theta_l$ . What’s more, in order to keep pace with convolution layers, we expanded the FIM of the fully connected layer in CNNs by a factor of  $\beta$  as described in Gao et al. (2020), where  $\beta = \max_{l \in \{\text{convolutional layers}\}} \{\max\{\text{tr}(\Theta_l), \vartheta\} / \dim(\Theta_l)\}$ . This damping technique for CNNs was first used in Gao et al. (2020). The purpose is to dynamically adjust the damping based on the FIM’s trace during training, so the damping can be adapted to the FIM’s elements to avoid the problem that the damping is large enough to transform the second-order optimizer into the first-order one during training.

---

**Algorithm 1** TEKFAC algorithm

---

**Require:**  $\eta$  : learning rate

**Require:**  $\lambda$  : damping parameter

**Require:**  $\beta_1$  : exponential moving average parameter of the re-scaling factor  $\Theta_l$

**Require:**  $\beta_2$  : exponential moving average parameter of factors  $\Phi_l$  and  $\Psi_l$

**Require:**  $T_{\text{FIM}}, T_{\text{EIG}}, T_{\text{RE}}$  : FIM, eigendecomposition and re-scaling update intervals

$k \leftarrow 0$

Initialize  $\{\delta_l\}_{l=1}^L, \{\Phi_l\}_{l=1}^L, \{\Psi_l\}_{l=1}^L$  and  $\{\Theta_l\}_{l=1}^L$

**while** convergence is not reached **do**

**if**  $k \equiv 0 \pmod{T_{\text{FIM}}}$  **then**

    Update the factors  $\{\delta_l\}_{l=1}^L, \{\Phi_l\}_{l=1}^L$  and  $\{\Psi_l\}_{l=1}^L$  using Eq. (2.10)

**end if**

**if**  $k \equiv 0 \pmod{T_{\text{EIG}}}$  **then**

    Compute the eigenbasis  $Q_{\Phi_l}$  and  $Q_{\Psi_l}$  using Eq. (3.1), (3.7) and (3.9)

**end if**

**if**  $k \equiv 0 \pmod{T_{\text{RE}}}$  **then**

    Update the re-scaling factor  $\{\Theta_l\}_{l=1}^L$  using Eq. (3.2), (3.4) and (3.6)

**end if**

$\nabla_l^{(k)} \leftarrow (Q_{\Phi_l}^\top \otimes Q_{\Psi_l}^\top)^{(k)} \nabla_{\omega_l} h^{(k)}$

$\nabla_l^{(k)} \leftarrow \nabla_l^{(k)} / (\text{vec}(\Theta_l^{(k)} + \lambda I))$  (element-wise scaling)

$\nabla_l^{(k)} \leftarrow (Q_{\Phi_l} \otimes Q_{\Psi_l})^{(k)} \nabla_l^{(k)}$

$\omega_l^{(k)} \leftarrow \omega_l^{(k-1)} - \eta \nabla_l^{(k)}$

$k \leftarrow k + 1$

**end while**

---

For each layer, EKFac estimates the Kronecker factors  $A_{l-1}, U_l$  and the re-scaling factor  $(\Lambda_l^*)_{ii}$  using exponential moving average. Similarly, we can obtain the exponential moving average updates for TEKFAC in Eq. (3.3).

$$(\Theta_l)_{ii}^{(k+1)} \leftarrow \beta_1 (\Theta_l)_{ii}^{(k+1)} + (1 - \beta_1) (\Theta_l)_{ii}^{(k)}, \quad (3.6)$$

$$\Phi_l^{(k+1)} \leftarrow \beta_2 \Phi_l^{(k+1)} + (1 - \beta_2) \Phi_l^{(k)}, \quad (3.7)$$



$$\Psi_l^{(k+1)} \leftarrow \beta_2 \Psi_l^{(k+1)} + (1 - \beta_2) \Psi_l^{(k)}, \quad (3.8)$$

where  $\beta_1$  and  $\beta_2$  are two exponential moving average parameters of the re-scaling factor and Kronecker factors. Finally, TEKFACT updates the parameters by

$$\omega_l^{(k+1)} \leftarrow \omega_l^{(k)} - \eta(Q_{\Phi_l} \otimes Q_{\Psi_l})^{(k+1)} [(\Theta_l + \lambda I)^{(k+1)}]^{-1} (Q_{\Phi_l}^\top \otimes Q_{\Psi_l}^\top)^{(k+1)} \nabla_{\omega_l} h^{(k+1)}. \quad (3.9)$$

Drawing inspiration of EKFACT and TKFACT, we present TEKFACT. Using TEKFACT for training DNNs mainly involves: a) computing the TEKFACT eigenbasis by eigendecomposition; b) estimating the re-scaling factor  $\Theta_l$  as defined in Eq. (3.2); c) computing the gradient and updating model’s parameters. The full algorithm of TEKFACT is given in Algorithm 1, in which the Kronecker product can be computed efficiently by the following identity:  $(A \otimes U)\text{vec}(X) = \text{vec}(U^\top XA)$ .

### 3.2 Discussion of different methods

Because the scale of the curvature matrix for DNNs is too large, it is impractical to compute the exact curvature matrix and its inverse matrix for DNNs. In order to effectively use natural gradient descent in training DNNs, KFAC was firstly proposed in (Martens and Grosse, 2015), then EKFACT (George et al., 2018) and TKFACT (Gao et al., 2020) were presented gradually. In the last subsection, we propose TEKFACT. In this subsection, we will discuss the relationships and differences of these methods.

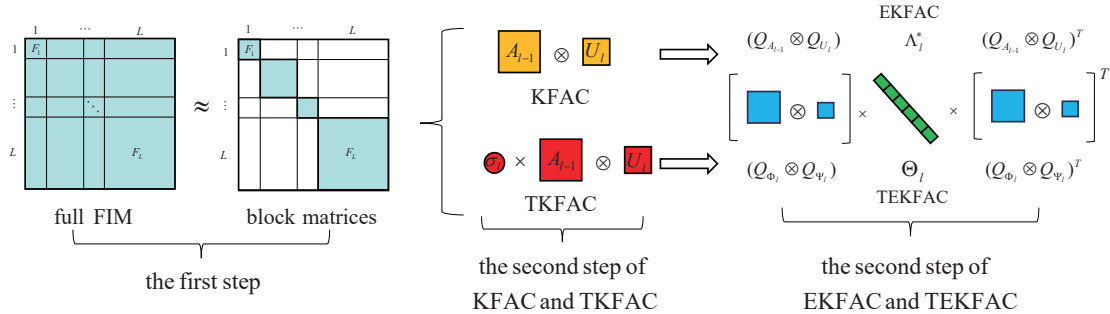


Figure 1: Illustration of the approximation process of KFAC, EKFACT, TKFACT and TEKFACT.

The approximation process of these methods can be divided into two steps. In the first step, they all decompose the FIM into block matrices according to layers of DNNs. By assuming that parameters of different layers are independent, the inverse of the full FIM is simplified as the inverse of these small block matrices. This step doesn’t make any difference for all these methods. In the second step, KFAC approximates different block matrices as the Kronecker product of two much smaller matrices, EKFACT reinterprets the KFAC by eigenvalue decomposition and corrects the inaccurate re-scaling factor under the KFAC eigenbasis, TKFACT approximates different block matrices as a Kronecker

product scaled by a coefficient, TEKFACT corrects the inaccurate re-scaling factor under the TKFAC eigenbasis based on the ideas of EKFACT. The two approximate processes of these methods are illustrated in Figure 1. We also summarize the different approximate models and re-scaling factors of these methods in Table 1.

Table 1: Summary of some optimizers

optimizer	$F_l$	re-scaling factor
KFAC(Martens and Grosse, 2015)	$A_{l-1} \otimes U_l$	$\Lambda_{A_{l-1}} \otimes \Lambda_{U_l}$
EKFAC(George et al., 2018)	$A_{l-1} \otimes U_l$	$\text{diag}(\mathbb{E}[\text{tr}((Q_{A_{l-1}} \otimes Q_{U_l})^\top \nabla_{\omega_l} h)^2])$
TKFAC(Gao et al., 2020)	$\sigma_l \Phi_l \otimes \Psi_l$	$\sigma_l (\Lambda_{\Phi_l} \otimes \Lambda_{\Psi_l})$
TEKFAC	$\sigma_l \Phi_l \otimes \Psi_l$	$\text{diag}(\mathbb{E}[\text{tr}((Q_{\Phi_l} \otimes Q_{\Psi_l})^\top \nabla_{\omega_l} h)^2])$

In TKFAC, an important property is to keep the traces equal before and after the approximation. For TEKFACT, this property can be still kept because

$$\begin{aligned}
 \text{tr}(F_l^{(\text{TEKFAC})}) &= \text{tr}((Q_{\Phi_l} \otimes Q_{\Psi_l}) \Theta_l (Q_{\Phi_l} \otimes Q_{\Psi_l})^\top) = \text{tr}(\Theta_l) \\
 &= \sum_i (\Theta_l)_{ii} = \sum_i \mathbb{E}[\text{tr}((Q_{\Phi_l} \otimes Q_{\Psi_l})^\top \nabla_{\omega_l} h)_i^2] \\
 &= \text{tr}(\mathbb{E}[(Q_A \otimes Q_U)^\top \nabla_{\omega} h (\nabla_{\omega} h)^\top (Q_A \otimes Q_U)]) \\
 &= \text{tr}(\mathbb{E}[\nabla_{\omega} h (\nabla_{\omega} h)^\top]) = \text{tr}(F_l),
 \end{aligned}$$

where  $F_l^{(\text{TEKFAC})}$  represents the approximation defined by Eq. (3.3) and  $F_l$  is the exact FIM. Similar to this conclusion, EKFACT can also keep the traces equal. However, we should note that EKFACT is based on the KFAC (Eq. (2.4)) and correcting the re-scaling factor, then the traces can be kept equal. TKFAC proposes a different approximation (Eq. (2.8)) and uses a trace operator to get the calculation formula under the condition that the trace is equal. The motivations for EKFACT and TKFAC are different. Finally, the relationships among these methods are summarized in Figure 4.

## 4 Experiments

To show the effectiveness of TEKFACT, we empirically demonstrate its performance on several standard benchmark datasets for some deep CNNs. Experimental results are given in the following subsection.

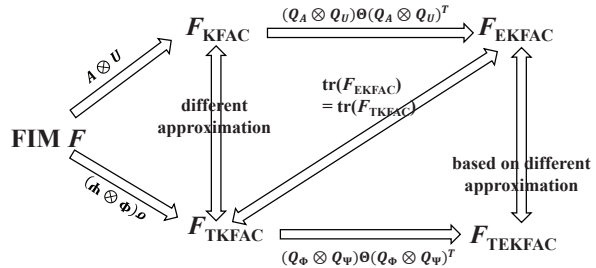


Figure 2: Illustration of the relationships of KFAC, EKFACT, TKFAC and TEKFACT.

## 4.1 Setup

**Datasets and models:** In this paper, we employ three commonly used image classification datasets: CIFAR-10, CIFAR-100 (Krizhevsky et al., 2009) and SVHN (Netzer et al., 2011). These datasets all consist of colored images with  $32 \times 32$  pixels. More details of these datasets are described in Table 2. We adopt a standard data augmentation scheme including random crop and horizontal flip for CIFAR-10/100, and we do not use data augmentation for SVHN. We consider the performance of different methods on two widely used deep CNNs: VGG16 (Simonyan and Zisserman, 2014) and ResNet20 (He et al., 2016).

Table 2: Statistics of the datasets used in experiments.

Dataset	#classes	#training set	#testing set
CIFAR-10	10	50000	10000
CIFAR-100	100	50000	10000
SVHN	10	73257	26032

**Baselines and hyper-parameters selection:** Our method mainly modify the EK-FAC eigenbasis according to the model adopted in TKFAC, so we mainly focus on the performance of TEKFAC compared with EK-FAC and TKFAC. Therefore, we choose SGDM, Adam, EK-FAC and TKFAC as baselines. We mainly refer to the parameters setting <sup>1</sup> <sup>2</sup> in recent related articles (Bae et al., 2018; Gao et al., 2020; Zhang et al., 2019). For all experiments, the hyper-parameters are tuned as follows:

- learning rate  $\eta$ :  $\{1e-4, 3e-4, 1e-3, 3e-3, 1e-2, 3e-2, 1e-1, 3e-1, 1, 3\}$ . The initial learning rate is multiplied by 0.1 every 20 epochs for SVHN and every 40 epochs for CIFAR10/100.
- damping  $\lambda$ :  $\{1e-8, 1e-6, 1e-4, 3e-4, 1e-3, 3e-3, 1e-2, 3e-2, 1e-1, 3e-1\}$ .
- the parameter to restrict trace  $\vartheta$ :  $\{1e-4, 1e-3, 1e-2, 1e-1, 1, 10, 100\}$ .
- moving average parameter  $\beta_1, \beta_2$ :  $\beta_1 = \beta_2 = 0.95$ .
- momentum: 0.9.
- $T_{\text{FIM}} = T_{\text{EIG}} = 50, T_{\text{INV}} = 200$ .
- batch size: 128 for SVHN, CIFAR-10/100.

For all methods, we use batch normalization and don't use weight decay. All experiments are run on a single RTX 2080Ti GPU using TensorFlow and repeated three times.

<sup>1</sup><https://github.com/pomonam/NoisyNaturalGradient>

<sup>2</sup><https://github.com/gd-zhang/Weight-Decay>

## 4.2 Results of experiments

**Results of CIFAR-10, CIFAR-100 and SVHN:** We perform extensive experiments on three standard datasets to investigate the effectiveness of TEKFACT. The main results on SVHN and CIFAR10/100 are shown in Figure 3 and Table 3. Figure 3 shows the results of SGDM, Adam, EKFACT, TKFACT and TEKFACT on these three datasets in terms of testing accuracy. In Figure 3, we can see that all the second order optimizers (EKFACT, TKFACT and TEKFACT) converge faster than SGDM and Adam. On SVHN and CIFAR-10, TEKFACT achieves same or faster convergence as TKFACT (faster than EKFACT clearly on all datasets) while achieving better accuracy. On CIFAR-100, although TEKFACT converges slower in the first few epochs, it can achieve same convergence as TKFACT after about 30 epochs with better accuracy. The final testing accuracies are summarized in Table 3.

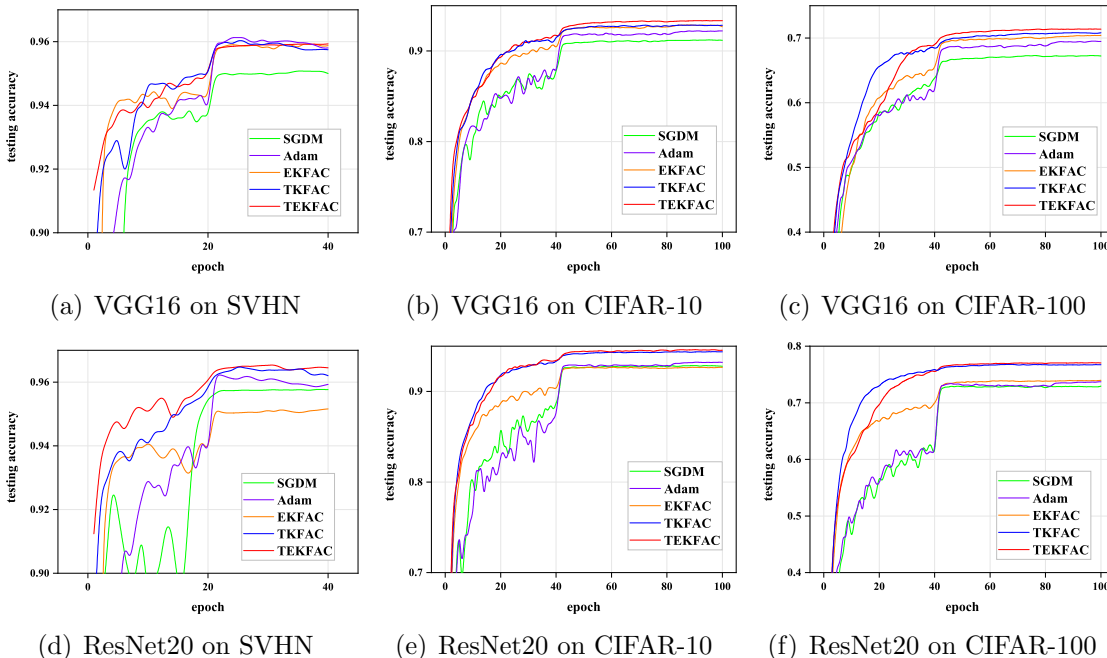


Figure 3: The curves of testing accuracy with epochs for SGDM, Adam, EKFACT, TKFACT and TEKFACT on SVHN, CIFAR-10 and CIFAR-100. The models we used here are VGG16 and ResNet20. All results are repeated three runs and the curves show the average results.

Table 3 illustrates the testing accuracies of various methods (SGDM, Adam, EKFACT, TKFACT and TEKFACT) with different models (VGG16 and ResNet20) on the SVHN, CIFAR-10 and CIFAR-100 datasets. These experiments are repeated for three times and the results are reported in mean  $\pm$  standard deviation. As shown in Table 3, TEKFACT can achieve higher average accuracy than other baselines in all cases. Compared with EKFACT, TEKFACT greatly improves the testing accuracies of all datasets. For ex-

ample, TEKFAC improves 0.96% and 3.06% than EKFACT on the CIFAR-100 dataset. Compared with TKFAC, TEKFAC is also able to improve the testing accuracies. For TEKFAC, on the one hand, the idea of EKFACT is combined to correct the inexact re-scaling factor; on the other hand, the new approximation method and the effective damping technique proposed in TKFAC are considered, so a more effective algorithm is obtained. These results also illustrate this point.

Table 3: Results of the SVHN, CIFAR-10 and CIFAR-100 datasets on VGG16 and ResNet20 for SGDM, Adam, EKFACT, TKFAC and TEKFAC. We give the final testing accuracies (mean  $\pm$  standard deviation over three runs) after 40 epochs for SVHN and 100 epochs for CIFAR.

Dataset	Model	SGDM	Adam	EKFACT	TKFAC	TEKFAC
SVHN	VGG16	94.98 $\pm$ 0.09	95.80 $\pm$ 0.11	95.87 $\pm$ 0.13	95.75 $\pm$ 0.21	<b>95.93<math>\pm</math> 0.16</b>
SVHN	ResNet20	95.78 $\pm$ 0.15	95.93 $\pm$ 0.12	95.16 $\pm$ 0.07	96.20 $\pm$ 0.39	<b>96.45<math>\pm</math> 0.14</b>
CIFAR-10	VGG16	91.19 $\pm$ 0.15	92.21 $\pm$ 0.14	92.67 $\pm$ 0.22	92.83 $\pm$ 0.13	<b>93.35<math>\pm</math> 0.17</b>
CIFAR-10	ResNet20	92.79 $\pm$ 0.14	93.22 $\pm$ 0.18	92.66 $\pm$ 0.17	94.38 $\pm$ 0.04	<b>94.56<math>\pm</math> 0.12</b>
CIFAR-100	VGG16	67.29 $\pm$ 0.28	69.47 $\pm$ 0.25	70.41 $\pm$ 0.26	70.82 $\pm$ 0.12	<b>71.37<math>\pm</math> 0.18</b>
CIFAR-100	ResNet20	72.94 $\pm$ 0.11	73.70 $\pm$ 0.18	73.98 $\pm$ 0.21	76.73 $\pm$ 0.18	<b>77.04<math>\pm</math> 0.15</b>

**Sensitivity to hyper-parameters:** We also consider the performance of TEKFAC with different hyper-parameters. For TEKFAC, a parameter  $\vartheta$  is added to avoid the traces becoming too small during training as TKFAC, so the parameter  $\vartheta$  needs to be tuned during training. Therefore, we mainly consider the effect of the learning rate  $\eta$  and the parameter  $\vartheta$ . We present the results of TEKFAC with different settings on CIFAR-100 with ResNet20.

Table 4: Testing accuracies of different parameter  $\vartheta$  on CIFAR-100 with ResNet20 for TEKFAC.

Parameter $\vartheta$	0.0001	0.001	0.01	0.1
Testing accuracy	76.81 $\pm$ 0.28	76.65 $\pm$ 0.12	<b>77.04<math>\pm</math> 0.15</b>	76.71 $\pm$ 0.17
Parameter $\vartheta$	1	10	100	
Testing accuracy	76.03 $\pm$ 0.26	74.74 $\pm$ 0.11	73.68 $\pm$ 0.09	

Table 4 shows the testing accuracies with different settings of  $\vartheta$ , where  $\vartheta$  is set to 0.0001, 0.001, 0.01, 0.1, 1, 10 and 100, respectively. The learning rate set to 0.001. Figure 4 shows the curves of the testing accuracies with epochs for different  $\vartheta$ . It is clear that the final testing accuracy is similar when  $\vartheta \in \{0.0001, 0.001, 0.01, 0.1\}$ . However, the testing accuracy decreases rapidly when  $\vartheta \geq 1$ . On the other hand, we can see that  $\vartheta$  also affects the speed of training from Figure 4. When  $\vartheta \in \{0.0001, 0.001, 0.01, 0.1, 1\}$ ,

TEKFAC converges slower but may have higher accuracy if  $\vartheta$  is smaller. When  $\vartheta \in \{10, 100\}$ , TEKFAC converges slowly and has lower accuracy. Therefore, we need to select  $\vartheta$  carefully to achieve good performance with the balance of training speed and final accuracy. For example, we choose  $\vartheta = 0.01$  on ResNet20 in this paper. Of course, 0.01 is not suitable for all networks, and  $\vartheta$  should be changed for different DNNs.

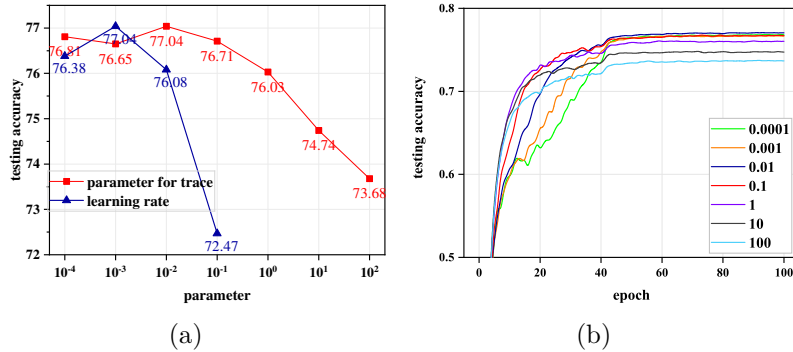


Figure 4: Results of different parameters. (a) The final testing accuracies of different parameter  $\vartheta$  and learning rate  $\eta$  with epochs for TEKFAC; (b) The curves of testing accuracies of different  $\vartheta$  with epochs for TEKFAC. The  $\vartheta$  is set to 0.0001, 0.001, 0.01, 0.1, 1, 10, 100 and  $\eta$  is set to 0.0001, 0.001, 0.01, 0.1.

Table 4 shows the testing accuracies with different settings of the learning rate  $\eta$ , where  $\eta$  is set to 0.0001, 0.001, 0.01, and 0.1, respectively. The parameter  $\vartheta$  is set to 0.01. We can see that the learning rate also has a great influence on the results of TEKFAC. For CIFAR-100 on ResNet20, 0.001 is a good selection.

Table 5: Testing accuracies of different learning rate  $\eta$  on CIFAR-100 with ResNet20 for TEKFAC.

Learning rate $\eta$	0.0001	0.001	0.01	0.1
Testing accuracy	$76.38 \pm 0.15$	<b><math>77.04 \pm 0.15</math></b>	$76.08 \pm 0.14$	$72.47 \pm 0.23$

## 5 Conclusions

Inspired by the idea of EKfAC and the new approximation of natural gradient adopted by TKfAC, we proposed TEKFAC algorithm in this work. It not only corrected the inexact re-scaling factor under the TKfAC eigenbasis but also changed the EKfAC eigenbasis based on the new approximation. The relationships of recent methods have also been discussed. Experimental results showed that our method outperformed SGDM, Adam, EKfAC and TKfAC. Of course, the performance of our method on other DNNs or more complex large-scale training tasks needs to be further studied.

## References

- Shun-Ichi Amari. Natural gradient works efficiently in learning. *Neural Computation*, 10(2):251–276, 1998.
- Jimmy Ba, Roger Grosse, and James Martens. Distributed second-order optimization using kronecker-factored approximations. In *International Conference on Learning Representations*, 2017.
- Juhan Bae, Guodong Zhang, and Roger Grosse. Eigenvalue corrected noisy natural gradient. In *Workshop of Bayesian Deep Learning, Advances in Neural Information Processing Systems*, 2018.
- Albert S Berahas, Majid Jahani, and Martin Takáč. Quasi-Newton methods for deep learning: Forget the past, just sample. *arXiv preprint arXiv:1901.09997*, 2019.
- J. E. Dennis and Jorge J. Moré. Quasi-Newton methods, motivation and theory. *SIAM Review*, 19(1):46–89, 1977.
- John Duchi, Hazan Elad, and Singer Yoram. Adaptive subgradient methods for online learning and stochastic optimization. *Journal of Machine Learning Research*, 12(Jul): 2121–2159, 2011.
- Kaixin Gao, Xiaolei Liu, Zhenghai Huang, Min Wang, Zidong Wang, Dachuan Xu, and Fan Yu. Trace-restricted kronecker factorization to approximate natural gradient descent for convolution neural networks. *arXiv preprint arXiv:2011.10741*, 2020.
- Thomas George, César Laurent, Xavier Bouthillier, Nicolas Ballas, and Pascal Vincent. Fast approximate natural gradient descent in a kronecker factored eigenbasis. In *Advances in Neural Information Processing Systems*, pages 9550–9560, 2018.
- Donald Goldfarb, Yi Ren, and Achraf Bahamou. Practical quasi-Newton methods for training deep neural networks. *arXiv preprint arXiv: 2006.08877v1*, 2020.
- Roger Grosse and James Martens. A kronecker-factored approximate fisher matrix for convolution layers. In *International Conference on Machine Learning*, pages 573–582, 2016.
- Kaiming He, Xiangyu Zhang, Shaoqing Ren, and Jian Sun. Deep residual learning for image recognition. In *Proceedings of the IEEE Conference on Computer Vision and Pattern Recognition*, pages 770–778, 2016.
- Diederik P Kingma and Jimmy Ba. Adam: A method for stochastic optimization. In *International Conference on Learning Representations*, 2014.
- Ryan Kiros. Training neural networks with stochastic Hessian-free optimization. In *International Conference on Learning Representations*, 2013.

- Alex Krizhevsky, Geoffrey Hinton, et al. Learning multiple layers of features from tiny images. 2009.
- Quoc V Le, Jiquan Ngiam, Adam Coates, Abhik Lahiri, Bobby Prochnow, and Andrew Y Ng. On optimization methods for deep learning. In *International Conference on Machine Learning*, pages 265–272, 2011.
- James Martens. Deep learning via Hessian-free optimization. In *International Conference on Machine Learning*, pages 735–742, 2010.
- James Martens and Roger Grosse. Optimizing neural networks with kronecker-factored approximate curvature. In *International Conference on Machine Learning*, pages 2408–2417, 2015.
- James Martens, Jimmy Ba, and Matt Johnson. Kronecker-factored curvature approximations for recurrent neural networks. In *International Conference on Learning Representations*, 2018.
- Yurii Nesterov. A method for solving the convex programming problem with convergence rate  $O(1/k^2)$ . *Soviet Mathematics Doklady*, 27(2):372–376, 1983.
- Yuval Netzer, Tao Wang, Adam Coates, Alessandro Bissacco, Bo Wu, and Andrew Y Ng. Reading digits in natural images with unsupervised feature learning. In *NIPS 2011 Workshop on Deep Learning and Unsupervised Feature Learning*, 2011.
- Kazuki Osawa, Yohei Tsuji, Yuichiro Ueno, Akira Naruse, Rio Yokota, and Satoshi Matsuoka. Large-scale distributed second-order optimization using kronecker-factored approximate curvature for deep convolutional neural networks. In *Proceedings of the IEEE Conference on Computer Vision and Pattern Recognition*, pages 12359–12367, 2019.
- Wenyong Pan, Kristopher A Innanen, and Wenyuan Liao. Accelerating Hessian-free Gauss-Newton full-waveform inversion via l-BFGS preconditioned conjugate-gradient algorithm. *Geophysics*, 82(2):R49–R64, 2017.
- J. Gregory Pauloski, Zhao Zhang, Lei Huang, Weijia Xu, and Ian T. Foster. Convolutional neural network training with distributed K-FAC. *arXiv preprint arXiv:2007.00784v1*, 2020.
- Ning Qian. On the momentum term in gradient descent learning algorithms. *Neural Networks*, 12(1):145–151, 1999.
- Herbert Robbins and Sutton Monro. A stochastic approximation method. *The Annals of Mathematical Statistics*, pages 400–407, 1951.
- Karen Simonyan and Andrew Zisserman. Very deep convolutional networks for large-scale image recognition. *arXiv preprint arXiv:1409.1556*, 2014.



Tijmen Tieleman and Geoffrey Hinton. Lecture 6.5-rmsprop: Divide the gradient by a running average of its recent magnitude. *COURSERA: Neural Networks for Machine Learning*, 4(2):26–31, 2012.

Minghan Yang, Dong Xu, Yongfeng Li, Zaiwen Wen, and Mengyun Chen. Sketchy empirical natural gradient methods for deep learning. *arXiv preprint arXiv:2006.05924*, 2020.

Guodong Zhang, Shengyang Sun, David Duvenaud, and Roger Grosse. Noisy natural gradient as variational inference. In *International Conference on Machine Learning*, pages 5847–5856, 2018.

Guodong Zhang, Chaoqi Wang, Bowen Xu, and Roger Grosse. Three mechanisms of weight decay regularization. In *International Conference on Learning Representations*, 2019.